Advances in High Energy Solid-State 2-micron Laser Transmitter Development for Ground and Airborne Wind and CO_2 Measurements

Upendra N. Singh[1], Jirong Yu[1], Mulugeta Petros[2], Songsheng Chen[1], Michael J. Kavaya[1], Bo Trieu[1], Yingxin Bai[3], Paul Petzar[4], Edward A. Modlin[1], Grady Koch[1] and Jeffrey Beyon[1]

[1]NASA Langley Research Center, Hampton, VA 23681 USA
[2]Science and Technology Corporation, 10 Basil Sawyer Drive, Hampton, VA 23666 USA
[3]SSAI, One Enterprise Parkway, Suite 300, Hampton, VA 23666 USA
[4]National Institute of Aerospace, Hampton, VA 23666 USA

ABSTRACT

Sustained research efforts at NASA Langley Research Center (LaRC) during last fifteen years have resulted in a significant advancement in 2-micron diode-pumped, solid-state laser transmitter for wind and carbon dioxide measurement from ground, air and space-borne platform. Solid-state 2-micron laser is a key subsystem for a coherent Doppler lidar that measures the horizontal and vertical wind velocities with high precision and resolution. The same laser, after a few modifications, can also be used in a Differential Absorption Lidar (DIAL) system for measuring atmospheric CO_2 concentration profiles. Researchers at NASA Langley Research Center have developed a compact, flight capable, high energy, injection seeded, 2-micron laser transmitter for ground and airborne wind and carbon dioxide measurements. It is capable of producing 250 mJ at 10 Hz by an oscillator and one amplifier. This compact laser transmitter was integrated into a mobile trailer based coherent Doppler wind and CO_2 DIAL system and was deployed during field measurement campaigns. This paper will give an overview of 2-micron solid-state laser technology development and discuss results from recent ground-based field measurements.

Keywords: Diode-pumped lasers, Solid state laser, Doppler wind lidar, Space lidar, CO_2, Airborne lidar, Differential Absorption Lidar

1. INTRODUCTION

The 2-micron lidar technology development being pursued at NASA LaRC is critical to satisfy one of the National Research Council (NRC) 2007 Earth Science Decadal Survey earth science missions recommended to NASA, and is a potential candidate for a second recommended mission. It is the leading candidate for the "3D-Winds" mission[1], and is a potential candidate for space-based CO_2 measuring mission called ASCENDS[1] using the same laser technology with the Differential Absorption Lidar (DIAL) technique. The future could possibly also include wind and CO_2 simultaneously from one lidar.

Solid-state 2-micron laser is a key subsystem for a coherent Doppler lidar that measures the horizontal and vertical wind velocities with high precision and resolution [1]. The same laser, after a few modifications, can also be used in a Differential Absorption Lidar (DIAL) system for measuring atmospheric CO_2 concentration profiles [2]. Development of a high energy, high efficiency, high beam quality, single frequency, compact and reliable solid state 2-micron laser is critically needed for such lidar systems. Although the capability of producing multi-joule energy by 2-micron solid state lasers was predicted a decade ago [3], the significant advancements in the high energy 2-micron laser demonstration have not been achieved until recently. A 400mJ Q-switched 2-micron laser system using a conductively cooled laser pump module was reported in 2004 [4]. A 600 mJ Q-switched diode-pumped Tm:Ho:LuLF using a MOPA system at double pulse format was published in 2003 [5]. A Joule level 2-micron laser MOPA system was reported in 2004, but it was operated in double-pulse format [6, 7]. Conductively cooled 2-micron lasers recently have been demonstrated [8-10]. One of the approaches described in these papers transfers the heat generated by both pump diode lasers and laser crystal to heat sinks by heat pipes. This advanced thermal management provides efficient heat removal that the 2-micron laser requires. By passively cooling the laser, the

total efficiency of the laser system is significantly enhanced as well. It marked a significant milestone in the 2-micron laser development.

After 30 years of study, it is widely agreed by NASA, NOAA, the Integrated Program Office- National Polar-orbiting Operational Environmental Satellite Systems (IPO-NPOESS), and DOD scientists that the pulsed Doppler lidar is the best sensor to make the wind profile measurements. Space mission design studies have shown that using both coherent and direct detection Doppler wind lidars (CDWL and DDWL) in a "hybrid" Doppler wind Lidar (HDWL) approach results in lower overall power, mass, volume, and technology development risk as compared to trying to do the mission with either CDWL or DDWL. The reason is that the two DWL technologies share the job of vertical coverage of the atmosphere in HDWL. With HDWL, the CDWL does not need to have the large pulse energy and receiver optical diameter to overcome the steep decrease in aerosol backscatter as altitude increases. Similarly, the DDWL does not need the large average power (pulse energy x pulse rate) and receiver optical diameter to overcome the increasing atmospheric absorption as altitude decreases combined with stricter required velocity accuracy and vertical resolution requirements below 2 km. The NRC Decadal Survey endorsed the 3-D wind mission, the pulsed Doppler lidar sensor, and the HDWL approach[1]. HDWL was also endorsed by a recent NASA lidar technologies study[2]. The NRC Decadal Survey recommended an HDWL demonstration (science) mission in 2016 and an HDWL operational mission as early as 2022. The CDWL portion of the HDWL is identified as having 2-micron wavelength.

LaRC has been performing coherent detection lidar wind measurements and has been developing high-energy 2-micron pulsed laser technology for the space-based wind measurement for over 15 years. Laser development progress at NASA Langley Research Center (LaRC) under the NASA's Earth Science Technology Office (ESTO) funded Laser Risk Reduction Program (LRRP) has eliminated a large amount of risk for NASA's goal of global wind measurement.

In the 1980s the largest demonstrated 2-micron pulse energy was 20 mJ, while simulations showed a requirement of 20 J with a 1.5 m diameter telescope for coherent-detection space-based global winds. The pulse energy deficit of a factor of 1000 was very daunting and the mission was deemed high risk. The 2-micron laser group at NASA LaRC worked to increase the pulse energy while also working on the important space mission considerations of high efficiency, excellent beam quality, narrow pulse spectrum, long lifetime, compact packaging, and space qualification. The technique of measuring wind was to be coherent-detection Doppler lidar. This high velocity accuracy, high sensitivity technique required excellent beam quality for sufficient signal, and narrow pulse spectrum for high accuracy.

The LaRC team worked on several fronts and made continuous progress. The LaRC team demonstrated 700 mJ at 1 Hz pulse repetition frequency (PRF) with 5 laser amplifiers in 1996; and 600 mJ at 10 Hz with 4 amplifiers in 1997. These laser designs all used liquid cooling for both the laser diode arrays (LDAs) and the laser rod. They subsequently demonstrated 355 mJ at 2 Hz with 1 amplifier and the novel Ho:Tm:LuLF laser material with the new conductively cooled LDA laser head design in 2002; 95 mJ at 10 Hz with no amplifiers (pulsed oscillator only) in 2003; 1200 mJ at 2 Hz with 2 amplifiers in 2005; and 355 mJ at 10 Hz with one amplifier and the new AA package LDAs in a compact package in 2007. Prior to 2007, the A package LDA had been used.

A parallel effort to design a fully conductively cooled laser head design produced 400 mJ at 5 Hz with one amplifier in 2007. This was very important since a laser for space needs to be all conductively cooled. The fully conductively cooled lasers permitted operation at much cooler temperatures. This led to the demonstration of much higher laser gain at lower temperatures. Another benefit to lower temperature operation is the ability to run both the LDA's and the laser rod at the same temperature rather than trying to keep them at different temperatures. In a teaming arrangement with one of the primary USA-based space-based laser developer, NASA LaRC researchers are transferring these breakthrough technologies for the development of two space-qualifiable laser transmitters to conduct the risk reduction efforts leading to qualify them for space operation. This Innovative Partnership Program (IPP) between government and industry, jointly funded by Earth Science Division at NASA HQ, LRRP program at LaRC Center, and the industry, will permit NASA developed technologies available to other federal agencies for future development of operational global wind profiling systems.

During these years the global wind mission design continued. Instead of coherent detection only, a "hybrid" Doppler lidar approach, consisting of coherent- and direct-detection Doppler lidars systems sharing the job of vertical coverage of the troposphere, was adopted. The coherent-detection pulse energy requirement dropped, by approximately a factor of 100, with this change (from 20 J to 200 mJ). The scanning was changed from continuous conical to step-stare conical with dwell time at each direction sufficient to use 60 coherent lidar shots for the measurement instead of 1. This changed dropped the pulse energy requirement about a factor of 8 (from 200 to 25 mJ). Later the step-stare conical scanner was changed to four fixed position 50-cm telescopes instead of one 150-cm diameter telescopes in order to eliminate the scanner's heavy moving parts. The smaller optical diameter raised the required pulse energy by approximately a factor of 10 (from 25 to 250 mJ). The situation has changed to a requirement of 250 mJ, with 1200 mJ already demonstrated, for a margin factor of 4.8. For pulse energy alone, moving from a x1000 deficit to a x4.8 margin represents a tremendous reduction in mission risk.

With support from NASA Laser Risk Reduction Program (LRRP) and Instrument Incubator Program (IIP), NASA Langley Research Center has developed a state-of-the-art compact lidar transceiver for a pulsed coherent Doppler lidar system for wind measurement with an unprecedented laser pulse energy of 250-mJ in a rugged package. The novel high-energy, 2-micron, Ho:Tm:LuLiF laser technology developed at NASA Langley was employed to study laser technology currently envisioned by NASA for future global coherent Doppler lidar winds measurement. The 250 mJ, 10 Hz laser was designed, under NASA ESTO funded IIP proposal “Doppler Aerosol Wind Lidar (DAWN),” as part of an integral part of a compact lidar transceiver developed for future aircraft flight. Ground-based wind profiles made with this transceiver will be described. NASA Langley is currently funded to build complete Doppler lidar systems using this transceiver for the DC-8 aircraft in autonomous operation (DAWN Air-I and DAWN Air-II). Recently, LaRC 2-micron coherent Doppler wind lidar system was selected to contribute to the NASA Science Mission Directorate (SMD) Earth Science Division (ESD) hurricane field experiment in 2010 titled Genesis and Rapid Intensification Processes (GRIP). The 2-micron technology efforts at NASA LaRC towards NASA 3-D Winds Space Mission, showing past and currently funded program, is shown and summarized in Figure 1.

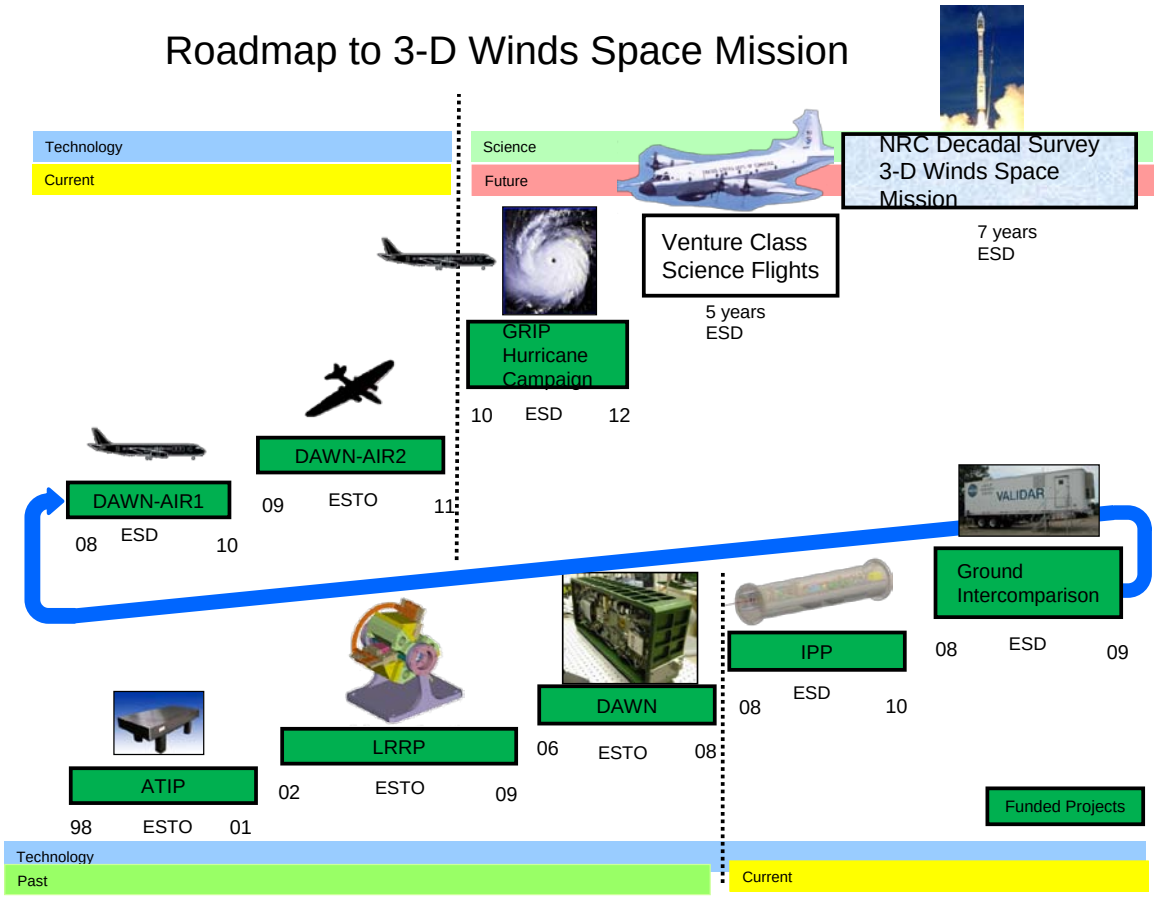

Figure 1. 2-micron Laser/Lidar technology development roadmap to 3-D Winds Space Mission

The following sections will describe the details of the 2-micron laser transmitter development in various stages for wind and CO_2 measurement application, compact packaging, integration of the laser transmitter into a complete coherent Doppler Wind and CO_2 DIAL system and results from the field measurements and intercomparison.

2. 1.2 JOULE PER PULSE Q-SWITCHED 2-µM LASER

The Master Oscillator Power Amplifier (MOPA) system is a typical way to achieve high energy, and at the same time to preserve good beam quality required by the nature of coherent lidars. Oscillator alone can't produce Joule level energy at 2-micron wavelength as severe optical damage can occur due to high fluence in the cavity. The MOPA 2-micron laser system comprises an oscillator and two power amplifiers.

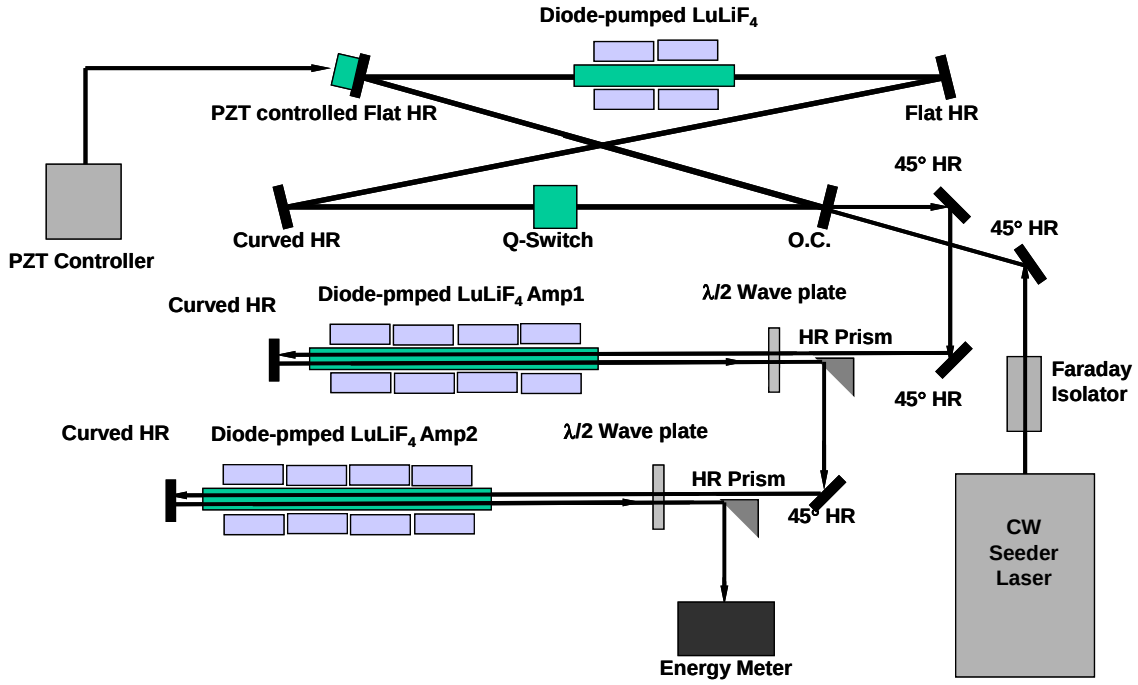

Figure 2. Schematics of 2-micron Master Oscillator and Power Amplifier (MOPA) system used for generating world record 1.2J energy/pulse.

The laser oscillator is similar to the one described in reference [11]. The oscillator and amplifier modules are all in monolithic design in which the laser rods are side-pumped by back-cooled conductive packaged GaAlAs diode laser arrays. The efficiency of the diode laser arrays is in the range of 38% to 44%. Recently, advancement of diode laser technologies led to higher than 50% efficiency for such quasi CW diode lasers. The diode arrays were directly mounted on aluminum modules, cooled by flowing water at 15°C. The pump diode arrays and the laser crystal rods are cooled in different chiller loops, so the temperatures of diodes and rods can be independently controlled.

The amplifier modules are similar to the oscillator module design, except using four banks of three, radially arranged laser pump diode arrays with total nominal pump energy of 7.2J of 1ms pulses. The symmetry afforded

with side-pumped rod geometry helps to produce a high quality, circularly symmetric Gaussian beam output. The gain medium of the laser system is Tm:Ho:LuLF crystal with 6% Thulium and 0.5% Holmium doping concentration. A detailed study of the Tm:Ho co-doped crystals of YLF and the isomorphs LuLF and GdLF revealed that small changes in the thermal population of the lower laser level in ground state terminated lasers can significantly alter the laser performance [12]. The larger host ion size of Lu leads to larger crystal fields and, as a result, larger crystal field splitting of lanthanide series ions. Thus, the LuLF host crystals provide better laser performance compared with YLF or GdLF based lasers [13].

To obtain single longitudinal mode oscillation that a coherent Doppler wind lidar requires, an injection seeding technique is applied. This injection seeding is based on a ramp and fire technique. By injection seeding, not only a single longitudinal mode oscillator was obtained, but unidirectional output of the ring resonator was achieved as well. However, for simplifying this experiment, the injection seeding is not implemented. A retro reflector is used to obtain unidirectional output.

2-micron Ho lasers are quasi four level lasers, so low temperature of the laser gain medium helps to reduce the threshold and to increase the slope effciency. The coolant temperature can not be lower than 8°C in the experiment, limited by the dew point constraint. The temperature is set at 8°C whenever the operation envirement allows.

To maximize the extracted energy, the two amplifiers shall be operated near saturation. Both of the amplifiers are configured at double pass to increase amplifier efficiency. Under three-side pumping geometry, the gain profile peaked at the rod center and lower at edges. Some portion of the area around the edge of the rod where it did not directly face the diodes may not even reach the threshold of the population inversion, resulting in net loss in these areas. Thus, the optimal mode matching between the probe beam and the pump volume is an important factor. Mode matching is realized by selecting the radius of curvatures of the reflect mirrors between the amplifier stages such that the beam sizes at amplifiers are little larger than 3.0mm.

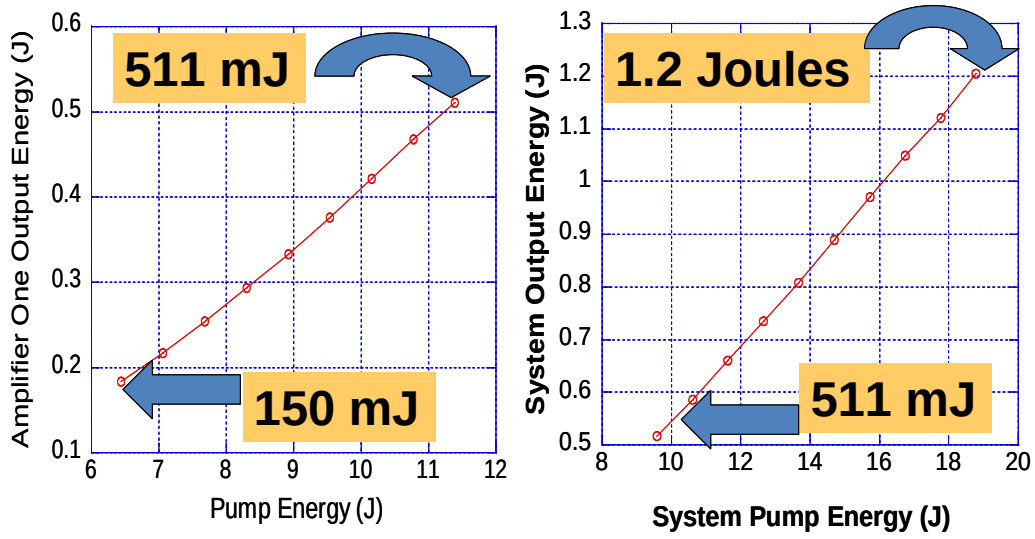

Figure 3. First and second amplifier performance in a double-pass configuration to amplify 150mJ/pulse energy from the seeded oscillator

Left plot in Fig. 3 depicts first amplifier performance for single Q-switch operations at a laser rod coolant temperature of 8°C. The probe energy from the oscilltor output is ~150mJ with full width half maximum of the pulse measured at 240 ns. The pump energy includes the combined oscillator and first amplifier pump diode incident energy. The amplifier did not produce gain until the pump energy increased to 4.03J. At the total maximum pump energy of 11.3J, 511mJ of output energy is obtained, representing an extracted energy of 361 mJ. Right plot in Figure 3 shows performance of second amplifier. The input energy for the second amplifier is 511 mJ.

With no pumping of second amplifier, only 93mJ passes through the amplifier due to ground state absorption. The optical transparency is achieved at pump energy of 3.759J, where the amplifier just overcomes the ground state absorption loss. For a total MOPA system pump energy of ~18.5J, 1.205 J of single Q-switched output energy is achieved. The optical to optical conversion efficiency is 6.5%. Energy extraction from the second amplifier is twice of the first amplifier under similar pump value. Nearly 700mJ energy is extracted from the second amplifier, compared to 361 mJ from the first.

Optical damage at the high energy output is a factor which needs be considered for reliable system operation. At the final beam output from amplifier two, the fluence is measured at ~26J/cm^2, which is comparable to the fluence level inside the oscillator cavity. Optical damage for the laser rod has been observed at a fluence level as low as ~30J/cm^2.

This 2-micron laser system provides nearly transform limited beam quality. The beam quality of the MOPA system is characterized by scanning knife edge technique measuring the beam diameters at 11 planes on both sides of the focus point for a 500mm focal length lens under full power condition. At the last amplifier stage, the beam quality is 1.4x transform limited.

3. ENGINEERING HARDENED 2-µM COHERENT DOPPLER WIND LIDAR TRANSCIEVER

In early years, research in the area of 2-µm laser technology for wind and carbon dioxide measurement were focused on primarily improving the efficiency and increasing the energy. Lately, with the funded work requiring system to be deployed in field for ground and airborne demonstration and validation, the effort has been focused on ruggedly package the state-of-the-art technology for mobile and airborne deployment. LaRC team has successfully developed a compact, engineered 2-micron coherent Doppler wind lidar transceiver and has ruggedized it for field deployment. This effort has resulted in five fold increase in laser power (energy x repetition rate) and tremendous reduction in size and mass from the previous implementation, as shown in Figure 4. The design of the lidar, summarized in Table 1, is similar to that described in a previous publication [14], with the addition of an optical amplifier to boost the energy of a 100-mJ laser oscillator to the 250-mJ level.

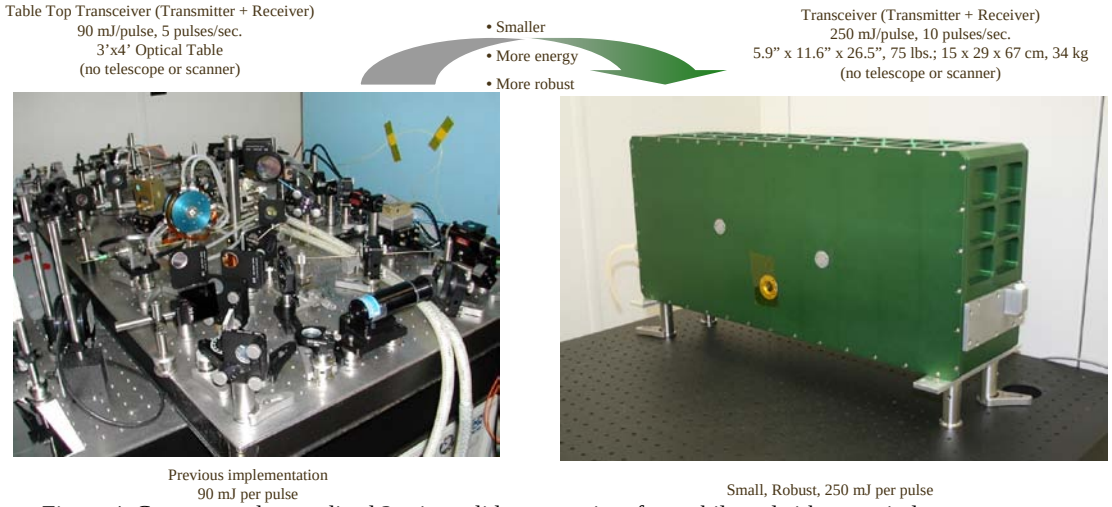

Figure 4. Compact and ruggedized 2-micron lidar transceiver for mobile and airborne wind measurement

As shown in Figure 5, the Coherent Doppler Wind Lidar (CDWL) system comprises: 1) the laser and optics subsystem, 2) the electrical and electronics subsystem, and 3) the data acquisition and computer subsystem. The laser and optics subsystem consists of the: 1) transmitter laser, 2) receiver, 3) transmit/receiver optical switch, 4) beam expanding telescope, and 5) scanner. The transmitter laser in turn comprises a CW injection or seed laser, the pulsed laser oscillator, the pulsed laser amplifier, and pump laser diode arrays for all three. The term "transceiver" is

used to mean the transmitter and receiver, but not the telescope, scanner, electronics, or computer. The transceiver components are outlined in blue color in Figure 5.

The laser architecture is Master Oscillator Power Amplifier (MOPA), and both the oscillator and single 2-pass amplifier are side pumped by AlGaAs AA-package Laser Diode Arrays (LDAs) emitting 792 nm light pulses 1 ms long. Three sets of two side by side LDAs are space at 120 degree intervals around the cylindrical laser rod. The LuLiF laser rod is doped with 6% Thulium (Tm) and 0.4% Holmium (Ho) rare earth atoms which replace Lutetium (Lu) atoms. The oscillator's 3-m long "bow tie" ring resonator utilizes 6 mirrors to achieve 8 reflections. An acousto-optic unit provides Q switching. A CW Ho:Tm:YLF laser serves as both the seed oscillator of the transmitter and the local oscillator of the receiver. A ramp and fire technique ensures the seed oscillator is matched to the resonator when it is fired by the Q-switch. Detection of the backscattered light begins with two InGaAs photodiodes arranged in a dual-balanced receiver configuration. The dual balanced approach eliminates any amplitude noise from the local oscillator and also eliminates the typical waste of a portion of the return signal and of the local oscillator.

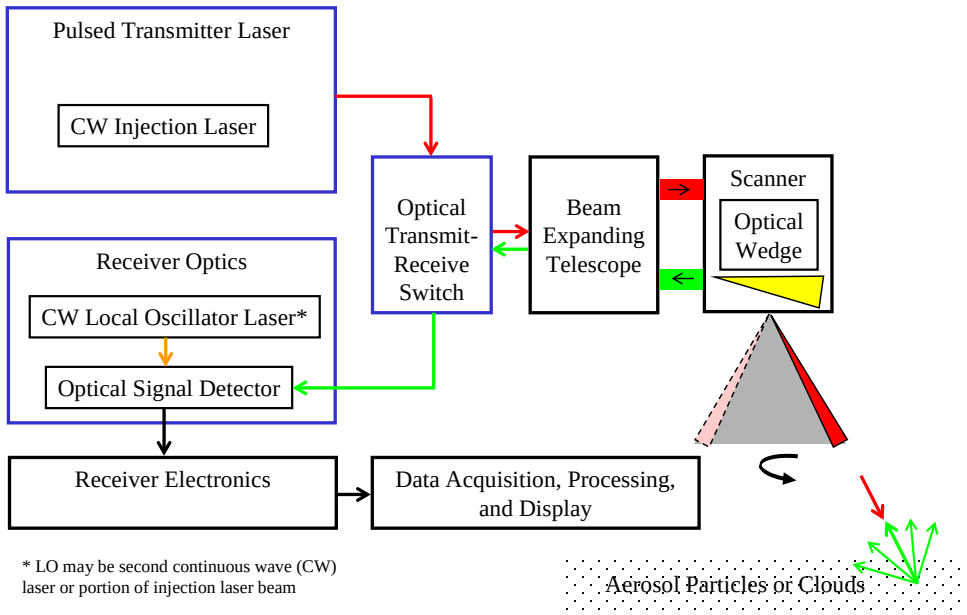

Figure 4. Block diagram of CDWL system in the downward looking, conical scanning configuration mode for airborne application.

The transceiver uses both sides of a temperature controlled rigid bench which is 9.5 x 21.75 x 1.25 inch (24 x 55 x 3 cm) before the optics are installed and 9.5 x 25.25 x 5.5 inch (24 x 64 x 14 cm) after the components are installed. One side of the bench consists of an injection seeded 2-micron oscillator and a power amplifier. The other side of the bench includes a seed laser, heterodyne receiver and laser health diagnostic components. All the optical mounts are custom designed and have space heritage. The laser beam height is 1 inch (2.54 cm). The enclosure around the optical bench is 11.5 x 26.5 x 6.4 inch (29 x 67.3 x 16.5 cm). The LDAs are cooled conductively just as they would be for a space mission. (In space the heat would flow to a radiator looking at cold space; on earth the heat is transferred to a fluid loop.).

The design specifications of this engineered transceiver are listed in table 1. This engineered transceiver consists of four lasers: a continue wave solid state seed laser at wave length of 2.053µm with linewidth at kilo Hz range, a power oscillator capable producing >100mJ/pulse energy, an amplifier operating at double pass configuration, and an alignment laser.

Table 1. Specifications of lidar.

Parameter	Value
Laser material	Ho:Tm:LuLiF
Pulse energy	250 mJ
Pulse width	200 ns
Pulse repetition rate	10 Hz
Spectrum	Single frequency
Wavelength	2053.5 nm
Beam quality (M^2)	< 1.3 times diffraction limit
Detector	InGaAs in dual-balanced configuration
Telescope aperture	15 cm
Scanner	8.5 inch aperture, full hemispherical coverage
Signal processing	500 Ms/s, 8-bits, real-time computation
Range resolution	153-m, overlapped 50%
Velocity resolution	1-m/s line of sight

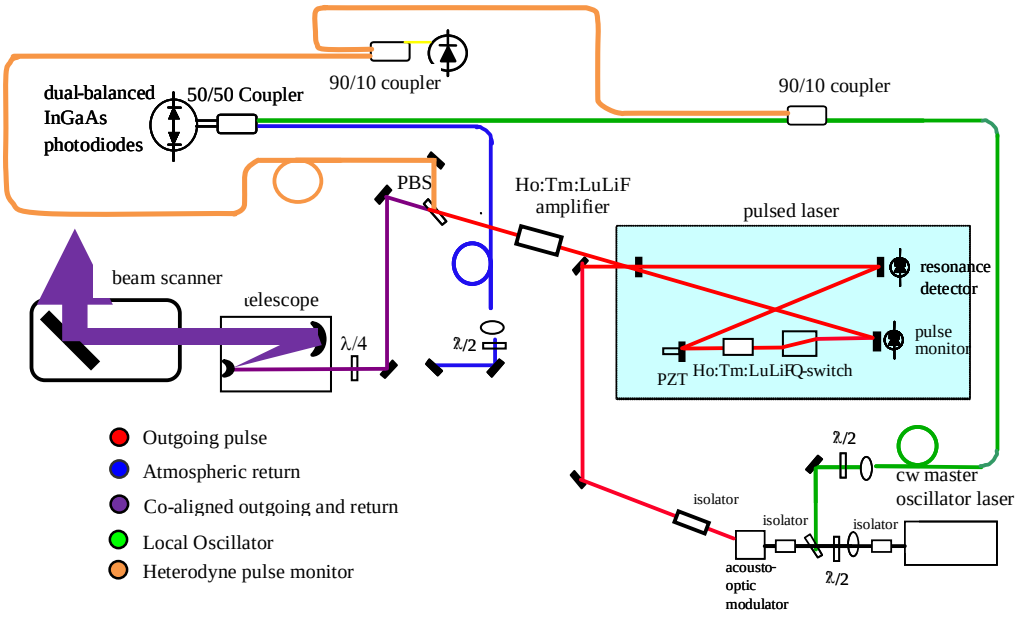

Fig. 5. Layout of the lidar.

The laser design has to meet high-energy as well as diffraction limited beam quality requirements; therefore, close attention is paid to the head design to avoid thermal distortion due to pump non-uniformity. Thermal distortion in the rod can have a detrimental effect on the beam quality. The radial side-pumping configuration and the uniform heat removal used here promote lower thermal distortion in the rod.

A traveling wave resonator design is chosen to avoid spatial hole-burning and facilitate single transverse mode operation. To meet the long pulse requirement, the oscillator length is set to 3 meters and formed with six mirrors having 8 bounces. The angles between the bounces are kept to a minimum. The mirrors on both sides of the oscillator are curved mirrors and are optimized to match the pump mode volume in the rod. The pump volume in the rod is derived from a Monte Carlo ray optics analysis which calculates the absorption flux in the rod.

Various curved mirrors were considered for the application. One of the design constraints for the oscillator design was the minimum aperture in the resonator should coincide with the Q-switch position. Although the Fused silica Q-switch has a 5mm transducer, the usable size is reduced to 3.3mm due to the Brewster angle. The TEM_{00} mode in the resonator is designed to have a large mode in the rod and a small mode in the Q- switch. A negative 3.2m lens was inserted to simulate the thermal lensing of the oscillator rod. The resonator design is calculated using ABCD matrix formalism.

The performance of the oscillator has been evaluated at different repetition rates and at different rod coolant temperatures. The maximum Q-switched output obtained ranges from 118mJ at 10Hz to 150mJ at 2Hz. Since the laser material is not a 4-level laser, it is sensitive to heat load; and hence the output drop at higher repetition rate is not totally unexpected. The plot in Figure 6 shows that there is still a considerable amount of energy left unused when the laser is in a single Q-switched output mode. The normal mode and the Q-switched energy have slope efficiency of 0.21 and 0.083, respectively.

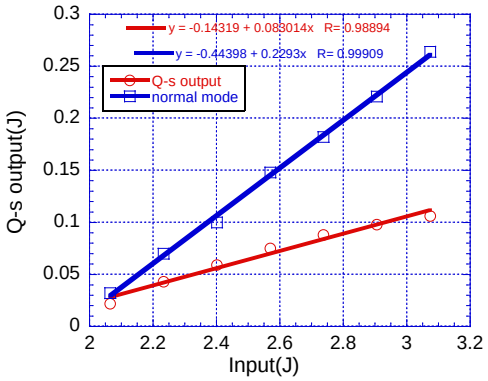

Figure 6. Oscillator performance at 10 Hz repetition rate

The oscillator output passes through a 2 meter focal length lens to set up a 3 mm beam at the input of the amplifier. Since c-axis of the amplifier rod is rotated to correct for the thermal distortion a half-wave plate is used to align the polarization. Using 100mJ as a probe beam from the oscillator, the double pass amplifier produced over 300 mJ. The result is shown Figure 5. At of 5°C with a double pass gain is slightly over 3. At a higher rod temperature of 8°C, the output energy was 275mJ. This was partially due to the reduction of the probe beam energy to 95 mJ, but the main reason is the thermal populating of the lower laser level. This shows the importance of depopulating the lower laser level for efficient operation.

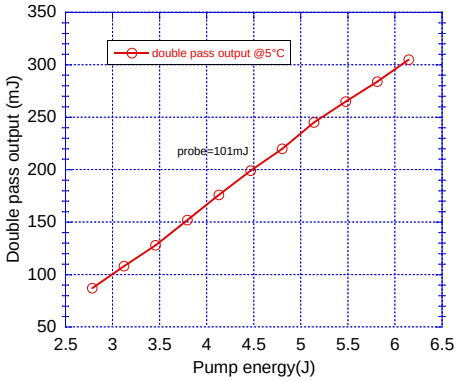

Figure 7 Double- pass amplifier output

A packaged transceiver shown in Figure 8 has achieved 114 mJ from the oscillator alone, and 300 mJ at 10 Hz from oscillator plus amplifier with excellent beam quality and the required long 180 ns pulse duration for the wind measurement.

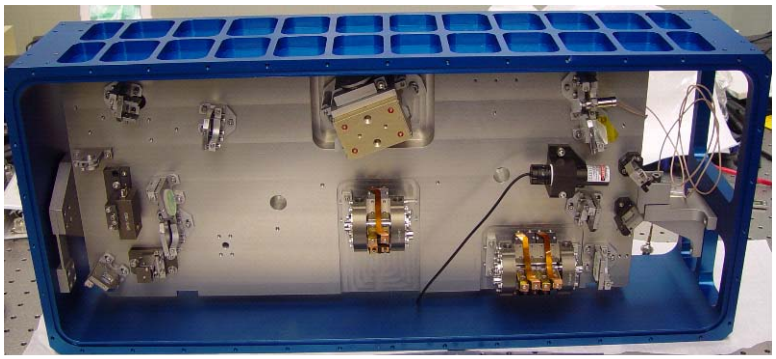

Figure 8. Photograph of Compact CDWL Transceiver in its Protective Enclosure.

To summarize the laser architecture, a Ho:Tm:LuLiF rod in a 3-m long cavity provides pulses at a 10 Hz rate. Injection seeding with a beam from a continuous-wave (CW) Ho:Tm:YLF laser creates a single-frequency output spectrum from the pulsed laser. Aside from providing an injection seed source, the CW laser is also used as a local oscillator for the receiver. The amplifier is a rod of Ho:Tm:LuLiF pumped from the side by 792-nm diode laser arrays providing a total pump energy of 7.2 J. After passing through a polarizing beam splitter, the output from the amplifier is directed toward a telescope of 15-cm primary aperture and 20x magnification. With this diameter the beam transmitted to the atmosphere is more than a factor of 10 under the maximum permissible exposure for pulsed lasers, making the output eye safe. A mirror positioned after the telescope deflects the beam vertically toward a beam scanner mounted through the roof of the laboratory. A quarter-wave plate is used before the telescope to create a circular polarization for transmission to the atmosphere. With reflection from aerosols assumed to create backscatter with the opposite sense polarization, the returned light is orthogonally polarized to the outgoing light. The polarizing beam splitter hence reflects the atmospheric return toward the receiver path. Received light is focused into an optical fiber and mixed with the local oscillator for heterodyning on InGaAs photodiodes in a dual-balanced configuration.

The sequence of operation is as follows. The scanner is commanded to turn to the desired direction. The laser is commanded to fire 10 times per second. Each time it fires only when the ramp and fire circuit indicate the injection laser is resonant with the pulsed laser cavity. Due to polarization of the light, the output pulse is directed by the optical transmit-receive switch to the beam expanding telescope, where the beam diameter is increased to 23 cm. The expanded beam is directed to the scanner where the optical wedge deflects the beam to be 45 degrees from the nadir direction with azimuth direction determined by the scanner. The transmitted pulse is backscattered by aerosol particles and cloud particles, causing a continuous return light signal vs. time. The return light at time t after the laser fires is from a segment of air that is at nominal range R from the lidar where the conversion factor is 150 m per microsecond, R = ct/2. The return light is reduced in diameter and directed to the optical signal detector. The detector is also illuminated by a portion of the CW injection laser to permit heterodyne detection. The receiver electronics condition the optical detector output for digitization and processing by the computer. Once in the computer, the user is free to process the data repeatedly for wind profiles with any desired combination of pulse accumulation, vertical resolution, frequency estimation algorithm, and assumed wind velocity search bandwidth.

Signal processing begins with digitization of the heterodyne signal at 500 Ms/s and 8-bit resolution. Digital signal processing chips parse the heterodyne signal into range bins, perform a Fourier transform on each bin, average across multiple pulses, and find the peak of the frequency spectrum to determine wind speed. In the data of the following sections, range bins of 512 samples are used with range bins overlapped by 50% to give line-of-sight wind

measurements every 76.8-m with 1-m/s speed resolution. Different pulse accumulation times are used depending on the measurement application. Multiple azimuths and associated line-of-sight wind measurements can be combined to find the horizontal wind vector as a function of altitude. All of the processing and wind data display is done in real time for immediate observation by an operator.

4. FIELD TEST SITE

For field testing, this lidar was installed within a mobile trailer designed for field deployment. Tests were conducted at a site run by Howard University in Beltsville, Maryland (39.05 N, 76.88 W). After the 180-mile trip from the lidar's home base in Hampton, Virginia the lidar transceiver maintained alignment. No adjustments to the lidar transceiver were needed over 5 weeks of measurements. Further alignment checks were made after the lidar's return home, again showing no degradation in optical alignment. This resistance to misalignment bodes well from the ultimate application of the lidar in which it will be installed in an aircraft. The test site was chosen for its accommodation of multiple visiting lidars and possession of many other meteorological sensors including wind measuring balloon sondes, sonic and propeller anemometers mounted on a tower, and a 915-MHz radio acoustic sounding system. Figure 2 shows a photograph of the lidar trailer, called VALIDAR, next to the Goddard Lidar Observatory for Wind (GLOW). GLOW is a 355-nm direct detection Doppler wind lidar. Joint measurements of the 2-μm coherent and 355-nm direct detection wind lidars were performed.

Fig. 9. Photograph of field test site at the Howard University Research Campus in Beltsville, Maryland. The 2-μm lidar is housed within a 35-foot long trailer testbed called VALIDAR. The other trailer houses the Goddard Lidar Observatory for Wind.

5. HORRIZONTAL AND VERTICAL WIND PROFILING

The horizontal wind vector is measured by steering the lidar beam to two perpendicular azimuths at a fixed elevation angle. Each azimuth angle is calibrated to a compass heading. With the wind speed versus altitude measured along both directions, the horizontal wind vector can be determined by vector summing the two components. The elevation angle is set at 45 degrees. 250 pulses were averaged at each azimuth. The beam was then steered toward a zenith view to measure the vertical wind with 250 pulses. This combination of horizontal and vertical wind measurement takes 3-minutes to complete for pulse accumulation and time for the beam scanner to move. The lidar signal processing computer repeats this scan pattern and records atmospheric data over a user-selected span, such as in the examples shown in Figure 10.

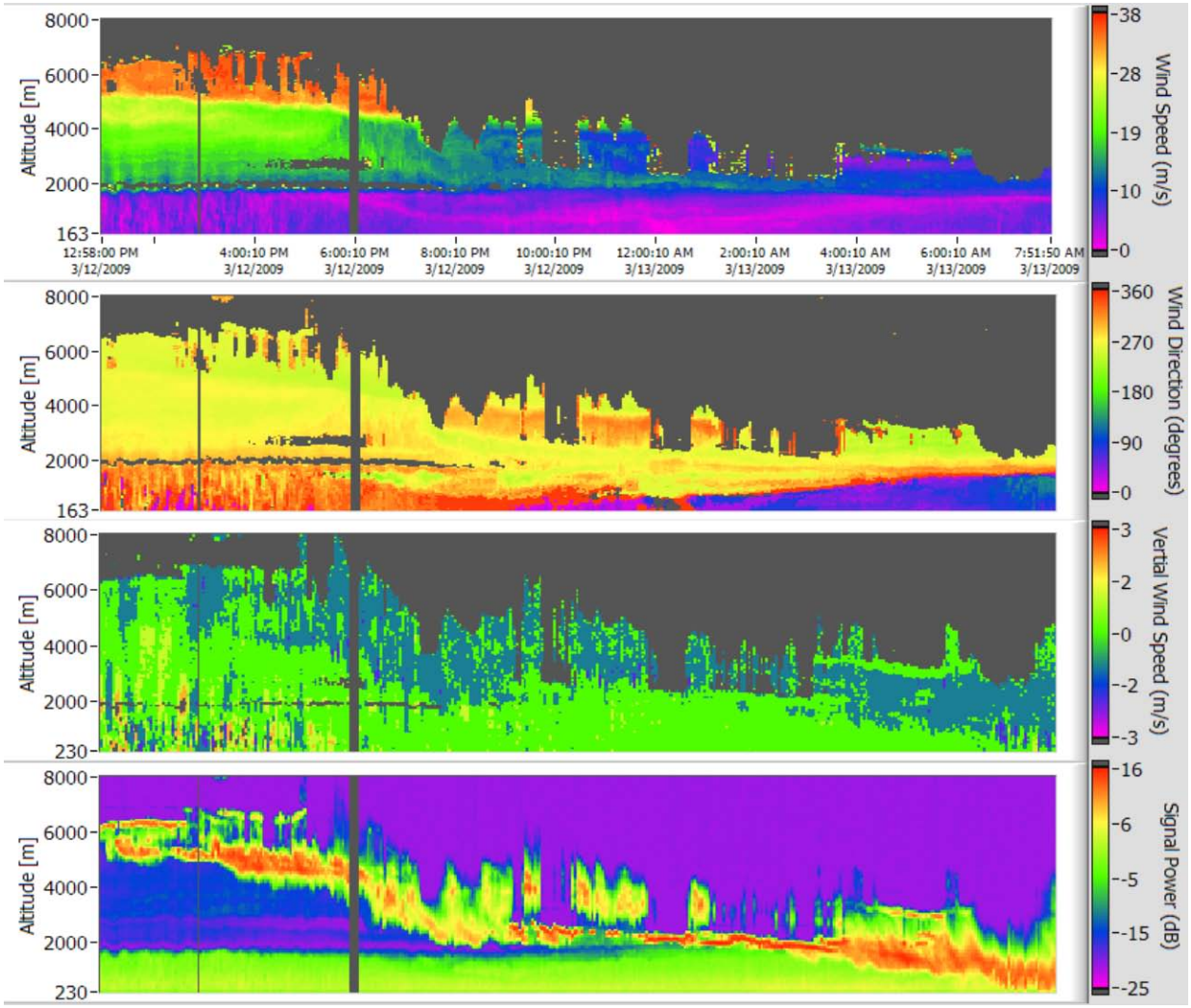

Fig. 10. Wind measurements made from a ground-based lidar during field testing in Beltsville, MD on March 12, 2009. The panels of data show, from top to bottom, the horizontal wind speed, the horizontal wind direction, the vertical wind speed, and signal power. The signal power panel indicates the presence of clouds and the relative density of aerosols. In this data set there is a complex cloud structure that comes to a very low cloud cover toward the end of the set. Despite the low cloud cover, wind measurements are made to an altitude of over 2-km. Throughout the 2nd half of the this data set, a frontal system passed through bringing rain—evidence of rain can be seen in the vertical wind motion. Features of interest are circled: (a) atmospheric boundary layer turbulence during daylight hours, (b) speed wind shear between the atmospheric boundary layer and free

troposphere, (c) directional wind shear between the atmospheric boundary layer and free troposphere, (d) change in wind direction as a frontal system passes through.

6. COMPARISON OF LIDAR AND BALLOON SONDE

Testing of the lidar also included measurements coincident with the launch of GPS balloon sondes. The balloon sonde provides correlated measurement with which to compare wind measurements and serves to demonstrate the lidar against a sensor that is widely used in the meteorological community. The balloons were Vaisala Radiosonde RS92 released approximately 1-km away from the lidar's location.

Four balloon launches were made on different days in February through March 2009. Figure 11 shows an example of one launch with the lidar and sonde results plotted together. The lidar measurements are in the same 3-minute scan pattern described in the previous section; though the vertical wind measurement is not used here (balloon sondes do not measure the vertical wind component). The lidar gives wind measurements continuously up to 5.2-km altitude, above which low aerosol backscatter begins to inhibit wind measurements.

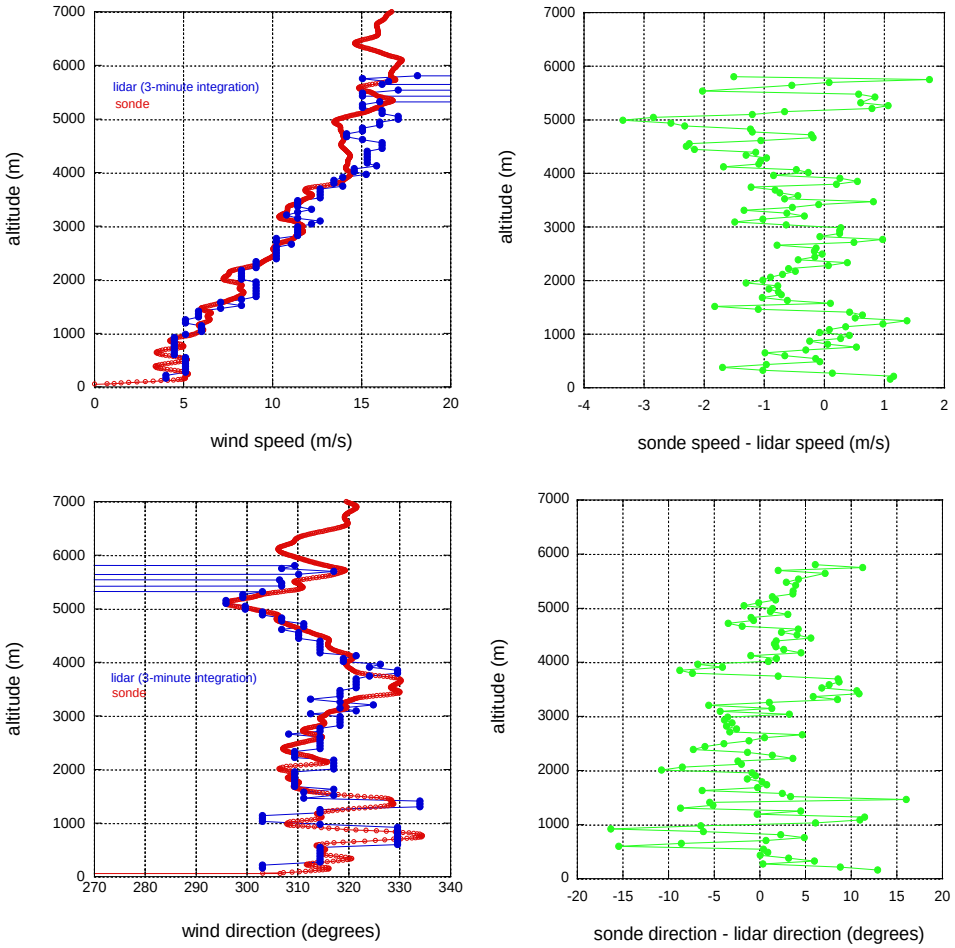

Fig. 11. Lidar and wind measurements co-plotted (left column) and residuals (right column).

The atmospheric boundary layer is evident in both measurements from the relatively low wind speeds at directions that change quickly with altitude below 1.5 km.

To assess the agreement between the two sensors, the difference between the sonde and lidar are also plotted in Figure 11. Specific range interval was used in the plots shown in Fig 11 to calculate a root-mean-square of the residuals gives 1.06-m/s for wind speed and 5.78-degrees for wind direction. In comparing the two sensors, there

are several differences in their characteristics that must be taken into consideration. First, the balloon takes a long time compared to the lidar to measure a profile. With a typical ascent rate of 5-m/s, for a balloon to reach 5-km altitude would take over 16 minutes. The lidar, on the other hand, creates a profile in a much shorter time (3-minutes in the scan format used here). In the comparison shown here the lidar profile used was recorded at the same time that the balloon was released. The balloon measurements at higher altitudes may occur at a time significantly later enough that the wind has changed. Second, the two sensors don't represent the same volume. The balloon is an *in-situ* sensor sampling a point at a time. The lidar represents a conical volume created as the beam is scanned in azimuth and uses a bin of range (153-m long in these measurements) to calculate a line-of-sight wind. Third, the balloon travels with the horizontal wind and travels over a different geographical point as it ascends. The lidar, in contrast, stays at the same point. Hence the differences found between the lidar and sonde of 1.06-m/s and 5.78-degrees have significant contributions from wind variation in time and over space aside from error sources from either sensor.

Field tests have thus demonstrated the maturation of high pulse energy 2-μm Doppler lidar. The lidar transceiver has been packaged in a rugged enclosure that withstands the vibration of transporting the instrument, temperature variation in a field environment, and operation without an operator present. Its 250-mJ output pulse energy gives wind measurements well into the free troposphere. The highest altitude at which horizontal wind measurements were made from aerosol backscatter ranged from a minimum of 5-km to a maximum 8.5-km over tests conducted in February and March 2009. While the tests conducted here were from the ground, the technology development goal is to make measurements from an aircraft. The transceiver described here is being integrated with a telescope and scanner in a vibration isolated; temperature controlled, and hermetically sealed enclosure for installation in aircraft. This lidar was integrated on DC-8 aircraft for participation in NASA Genesis and Rapid Intensification Processes (GRIP) hurricane field experiment during August-September, 2010. The results from GRIP campaign are in the process of being analyzed.

7. 2μM COHERENT DIFFERENTIAL ABSORPTION LIDAR TRANSMITTER (DIAL) FOR ATMOSPHERIC CO_2 SENSING

There is a great urgency to understand the process of CO_2 exchange in the context of global climate change. Knowledge of the spatial and temporal distribution in addition to the Natural and manmade sources/sinks in a global scale is crucial to predict and possibly manage the process. Most of the CO_2 measuring instruments, which contributed to the present knowledge base, are passive instruments that measure flux near the ground. In response to the challenges, laser based active instruments are being developed. These instruments rely on the measurements of the differential absorption between different wavelengths. Researchers at NASA Langley have been looking at this problem and have used an instrument initially designed as a wind coherent Doppler Lidar, to measure CO_2 flux [15-19]. The attractive feature of this instrument is that laser material with a long upper laser lifetime and as a result can produce two or more consecutive pulses within a few hundred microsecond spacing with a single pump pulse. This is an important consideration in terms of overall system design.

The operating wavelength around 2μm has a favorable weighting function near ground surface [20]. The R (30) CO2 line at 2050.967 nm (4875.75 cm-1) is selected for its temperature insensitivity, absorption strength and absence of absorption from other species [20, 22].

Similar efforts, as described in the earlier sections for developing a wind lidar transmitter, were undertaken for designing a double pulsed, injection seeded, and 2μm compact coherent DIAL transmitter for CO_2 sensing. This system was hardened for ground and airborne applications. The design architecture includes three seed lasers which provide controlled 'on and 'off' line seeding, injection seeded power oscillator and a single amplifier operating in double pass configuration. The active laser material used for this application is a Ho: Tm:YLF crystal and operates at the eye-safe wavelength of 2μm. The 3-meter long folded ring resonator produces 130-mJ with a temporal pulse length around 220 ns and 530ns pulses for 'on' and 'off' lines respectively. The separation between the two pulses is in the order of 200μs. The line width is in the order of 2.5MHz and the beam quality has an M^2 of 1.1 times diffraction limited beam. A final output energy for a pair of both 'on' and 'off' pulses as high as 315 mJ at a repetition rate of 10 Hz. The operating temperature is set around 20°C for the pump diode lasers and 10°C for the rod. Since the laser design has to meet high-energy as well as high beam quality requirements, close attention is paid

to the laser head design to avoid thermal distortion in the rod. A side-pumped configuration is used and heat is removed uniformly by passing coolant through a tube slightly larger than the rod to reduce thermal gradient. Double pulsing and injection seeding with two different frequencies to achieve a transform limited line width for DIAL application were attained.

8. CO_2 DIAL TRANSMITTER DESIGN

The transmitter architecture consists of a master oscillator and power amplifier system. With the amplifier operating in a double pass mode. The Locking, offsetting and the switching of the seed laser which is described in detail by Koch et al [14], is housed separately. This portion consists of three seed lasers. One locked to the Co_2 absorption center though a pressure controlled gas cell, in which the pressure is lowered 4 torr to narrow the absorption width for better discrimination. The second laser is offset from the center line by 4GHz from the absorption center. This is used as the 'on' line wavelength and routed to a switch along with a third laser tuned to 'off' line wavelength. The fiber based switch alternates the two wavelengths. The line width measurement of the seed laser is done by beating two similar lasers, the result showed a line width better than 13 KHz.

The lidar transmitter is housed in a sealed enclosure purged with dry air. The overall dimension of the system enclosure is 67cmX 16.5cmX26cm. It houses the optical bench which is populated on both sides. The oscillator and the amplifier are mounted on one side and local oscillator associated optics, and the receiver detectors on the other. The seed laser is fed in to the transmitter enclosure with a fiber feed through.

The bench is temperature controlled to avoid any thermal induced misalignment. All the optical mounts are designed to be adjustable, lockable and hardened to withstand vibrations that can occur in ground or airborne operation. The most important system requirements are shown in table 2.

Table2. Transmitter specifications

Laser material	Ho:Tm:YLF
Output energy (mJ)	192/125 on/off
Wavelength(μm) both pulses injection seeded	2.050125/ 2.050967
Repetition rate (Hz)	10/10 on/off
Pulse separation (μs)	~250
Pulse length(ns)	200/520
Line width(MHz)	<2.5
LO frequency offset(MHz)	105
Telescope aperture (cm)	15

Two features make this work unique from similar work presented before; the first is the seeding of the double-pulse with two different wavelengths within the 200μs and the other is the double pass amplifier that enabled high energy. The power oscillator is a three meter long ring resonator. The length is dictated by the narrow spectral line width requirement. And the ring configuration is to achieve a single transverse mode operation. The side pump volume and the TEM_{00} mode are closely matched to 2.3mm diameter.

The crystal is pumped with 3.2 Joules of 792nm pump radiation to produce 90mJ of single Q-switched output and 130mJ of double pulsed output. The Amplifier is twice the size of the oscillator and the pump energy is thus doubled.

The operation principle of Ho:Tm lasers is well understood[13, 22-25] and will only be briefly described here. In Ho:Tm:YLF the Tm ions are excited with 792 nm radiations from $^3H_6$ to $^3H_4$. A 6% Tm concentration is selected to secure self-quenching that warrants a quantum efficiency of close to 2. Thus for every photon absorbed in the Tm $^3H_4$ two atoms are produced in the Tm $^3F_4$ manifold. Tm $^3H_6$ is promoted to the Tm $^3F_4$ via non-radiative energy

transfer. Ideally, this results in 2 excitations in the Tm $^3F_4$ for every pump excitation in the Tm $^3H_4$. The actual quantum efficiency of this process is dependent on the Tm concentration and should approach 2 at high Tm concentrations. Lower Tm concentrations can promote other transitions which have deleterious effect; and higher Tm concentration raises the threshold without any added benefit. Energy is then transferred from $^3F_4$ to Ho $^5I_7$ and the 2 micron laser action occurs between the Ho $^5I_7$ and $^5I_8$. Since the Thulium is not directly involved in the actual 2 μm emission, the energy in the $^3F_4$ serves as a reservoir to repopulate the Holmium.

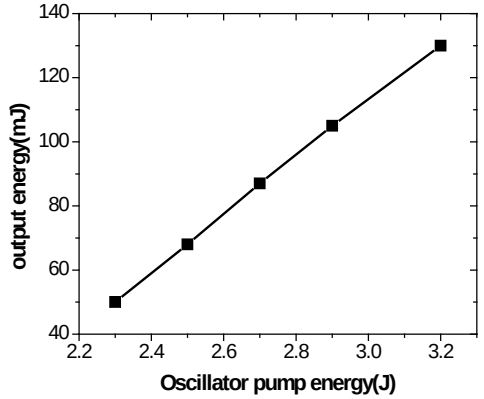

Figure 12. Oscillator performance

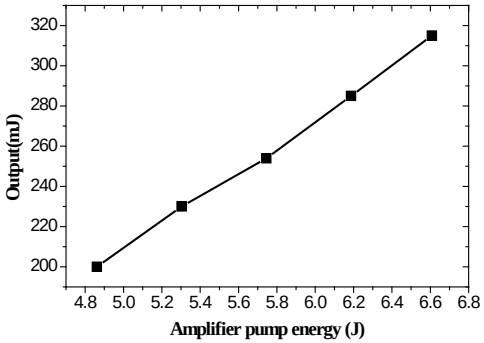

Figure 13. Amplifier performance

For DIAL application, most other systems use either two complete lasers or are forced to pump twice to produce two pulses within hundreds of microseconds. Ho:Tm:YLF operates much more efficiently in double pulse format than single pulse. Due to the long upper laser level life time and the energy stored in the Tm ion, the Holmium gets repopulated after the first Q-switch pulse. The second pulse is then extracted by simply opening the Q-switch. It has been shown that the energy ratio of the two pulses can be adjusted by controlling the first Q-switch time with respect pump pulse. The plot below represents the mechanism behind this phenomenon. The top trace represents a no lasing condition population continues to grow until a little after end of the pump pulse, typically 100μs and decays in 10 to 15ms. In single pulse operation, as soon as the Q-switch is fired and the population is depleted down to threshold, the Ho$^5I_7$ population then increases due to the rapid reduction the Ho$^5I_7$ population while the Tm $^3F_4$ population is intact. As a result, the Tm $^3F_4$ and Ho $^5I_7$ manifolds are no longer in quasi-thermal equilibrium. Thus the excited Tm ions in the $^3F_4$ manifold transfer the energy and repopulate the Ho ions until the Tm $^3F_4$ and Ho $^5I_7$ manifolds reach a quasi-thermal equilibrium again. This process takes about 150μs and results in the recovery of 50% of the depleted population at that moment the Q-switch can be fired again to extract additional energy.

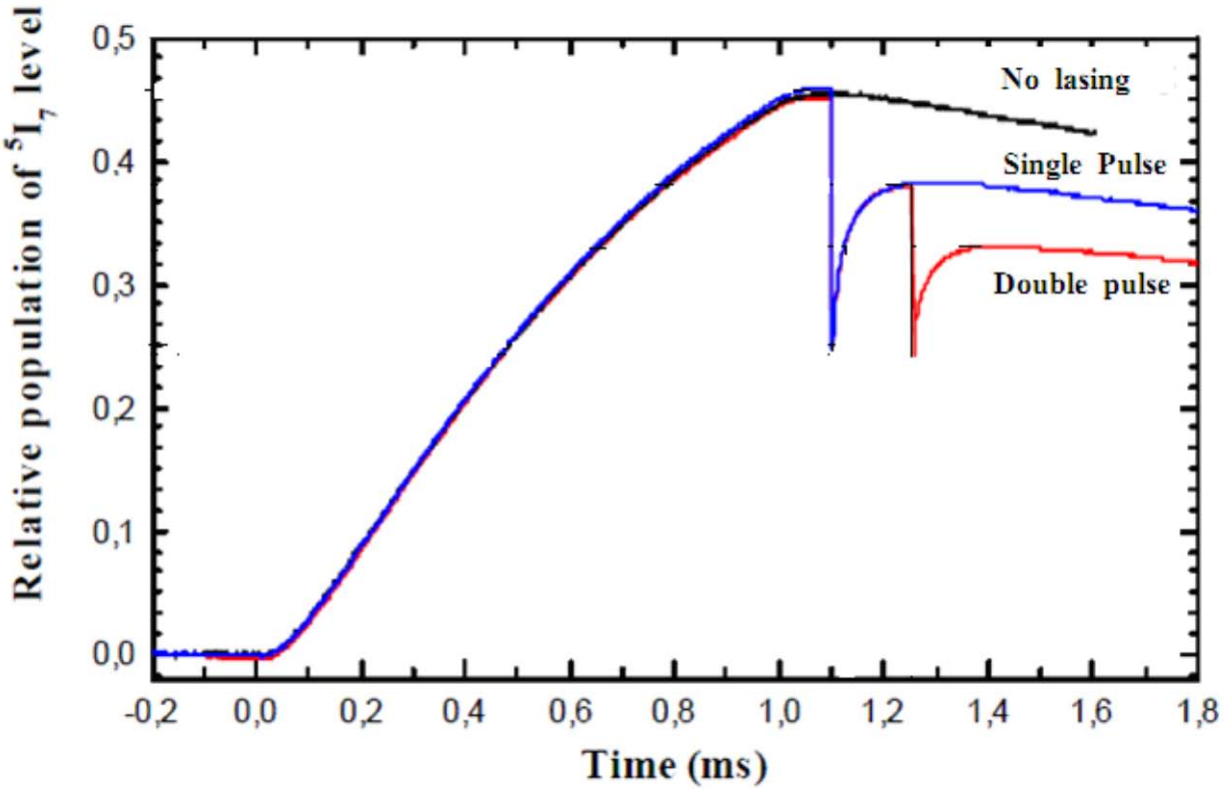

Figure 14. The relative population of the Ho upper laser level in three distinct conditions for 1ms pumps.

Seeding is achieved by a variation of ramp and fire scheme called push and pull method in which, the 'on' and 'off' line pulses are fired as the resonator mirror is pushed and pulled respectively. The seed laser is injected through the 75% reflective output coupler. Close to the laser gain peak, the length of the resonator is adjusted by pushing one of the resonator mirrors to produce a resonance signal at which time the 'on' line pulse is fired.

This wavelength dwells in the system to be used as local oscillator for the Lidar return. The length of this time is governed by the desired measurement range. If a 7.5km measurement is desired, the seed laser will be kept on for 50 microseconds before it is replaced by the 'off' line then the piezo-electric actuator pulls the length of the resonator to its original position providing another resonance peak for the 'off' line pulse.

The system has an inbuilt heterodyne monitoring system derived from the seed laser that is split using a 105MHz Acousto-optics modulator. The 0th order beam is used for generation of local oscillator which is routed via fiber optics to a monitor detector and a dual balanced return signal detector. The first order beam is routed to seed the laser thus providing an offset to the pulsed laser. Any scatter in the system is mixed to produce the diagnostic monitor signal. From which many aspects of the laser spectral characteristics can be determined. The measurements of the line width of each pulse shows both pulses produce near Fourier transform limit line width. The second pulse has a slightly narrow line width pertaining to its longer pulse length. A frequency jitter of +/- 1.5 MHz is measured on each of the pulses using heterodyne method. The FFT of this signal is measured and analyzed to look at the jitter over time. This same signal also provides the line width information at the FFT half power point. In addition, frequency chirp information can be extracted by splicing the heterodyne data and looking at the frequency at different places in the signal.

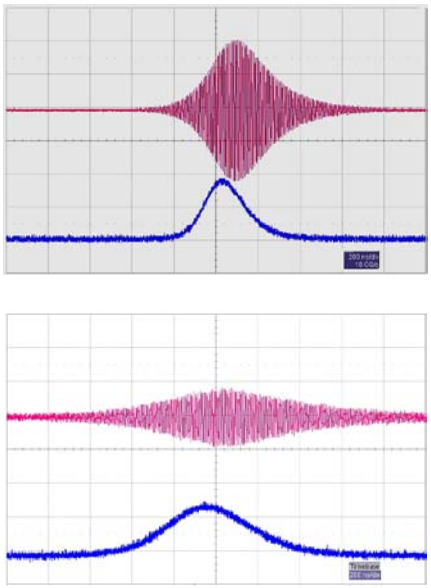

Figure 4a and b show the heterodyne signal of the local oscillator with the corresponding temporal pulse.

In summary, we have designed a Coherent DIAL instrument with high energy at 2μm and is ready to be fielded. This instrument is an important addition to the myriad of other instruments that are developed to measure the CO_2 concentration to the very high degree of accuracy required by the science objective.

9. CONCLUSIONS

Laser Risk Reduction Program (LRRP) and Instrument Incubator Program (IIP), NASA Langley Research Center has developed a state-of-the-art compact lidar transceiver for a pulsed coherent Doppler lidar system for wind measurement with an unprecedented laser pulse energy of 250-mJ in a rugged package. This high pulse energy is produced by a Ho:Tm:LuLiF laser with an optical amplifier. While the lidar is meant for use as an airborne instrument, ground-based tests were carried out to characterize performance of the lidar. Atmospheric measurements will be presented, showing the lidar's capability for wind measurement in the atmospheric boundary layer and free troposphere. Lidar wind measurements are compared to a balloon sonde, showing good agreement between the two sensors.

Similar architecture has been used to develop a high energy, Ho:Tm:YLF pulsed 2 μm Differential Absorption Lidar instrument based on coherent heterodyne technique that provides atmospheric CO2 measurements. Since aerosols are abundant in the atmospheric boundary layer, the pulse approach can determine CO2 concentrations as a function of distance with high spatial and temporal resolution, a valuable data product that is not currently available. This instrument will measure atmospheric CO2 profiles (by DIAL) initially from a ground platform, and then be prepared for aircraft installation to measure the atmospheric CO2 column densities in the atmospheric boundary layer (ABL) and lower troposphere. The airborne prototype CO2 lidar can measure atmospheric CO2 column density in a range bin of 1km with better than 1.5% precision at horizontal resolution of less than 50km.

10. ACKNOWLEDGEMENTS

This work was supported by Laser Risk Reduction Program, funded by NASA Earth Science Technology Office (ESTO) and NASA ROSES Wind Lidar Science Program of NASA Science Mission Directorate at NASA Headquarters, Washington, D.C.

11. REFERENCES

[1] W. E. Baker et al., "Lidar-Measured Winds from Space: A Key Component for Weather and Climate Prediction" Bull. Amer. Meteorol. Soc., Vol 76, No. 6, 869-888 (1995)

[2] Grady J. Koch, B. W. Barnes, M. Petros, J. Y. Beyon, F. Amzajerdian, J.Yu, R. E. Davis, S. Ismail, S. Vay, M. J. Kavaya and U. N. Singh, "Coherent differential absorption lidar measurements of CO2", Appl. Opts, Vol. 43, No. 26, 5092-5099 (2004)

[3] Mark E Storm, "Holmium YLF amplifier performance and the prospects for multi-Joule energies using diode-laser pumping", IEEE Journal of Quantum Electronics (ISSN 0018-9197), vol. 29, no. 2, p. 440-451, 1992

[4] M. W. Phillips and J. P. Tucker, Proc. SPIE, 5653, 146, (2004)

[5] Jirong Yu, Alain Braud and Mulugeta Petros, "600 mJ, Double-pulsed 2-micron laser" Opt. Lett., 28, 540 (2003)

[7] S. Chen, J. Yu, M. Petros, Y. Bai, B. C. Trieu, U. N. Singh and M. J. Kavaya, "Joule level Double-pulsed Ho:Tm:LuLF Master-Oscillator-Power-Amplifier (MOPA) for potential spaceborne lidar applications", Proc. SPIE, 5653, 175 (2004)

[8] K. Mizutani et al. "Development of conductive cooled 2-micron lasers", Proceeding 13th coherent laser radar conference, 32-35, 2005

[9] V. Sudesh, K Asai, K. Shimamura, T. Fukuda, "Pulsed Laser Action in Tm,Ho : LuLiF4 and Tm,Ho : YLiF4 Crystals Using a Novel Quasi-End-Pumping Technique", IEEE J. Quant. Electronics, 38, 1102 (2002)

[10] M. Petros, J. Yu, Tony Melak, B. C. Trieu, S. Chen, U. N. Singh and Y. Bai, "High energy totally conductive cooled, diode pumped, 2μm laser", in OSA Trends in Optics and Photonics Series (TOPS) vol. 98, Advanced Solid state Photonics, Craig Denman and Irina Sorokina, ed. DC 2005, pp 623-627

[11] B. C. Trieu, Jirong Yu, M. Petros, Luis Ramos-Izquierdo, Glenn Byron, Perk Sohn, Yingxin Bai, S. Chen, U. N. Singh, M. J. Kavaya, "Design of a totally conductive cooled, diode pumped 2-micron amplifier", Proc. SPIE 5887, p. 5887OM-1-5887OM-11, 2005

[12] Jirong Yu, U. N. Singh, N. P. Barnes and M. Petros, "125-mJ diode-pumped injection-seeded Ho;Tm:YLF laser" Opt. Lett. 23,780 (1998)

[13] Brian M. Walsh, Norman P. Barnes, Mulugeta Petros, Jirong Yu , Upendra N. Singh, " Spectroscopy and modeling of solid state lanthanide laser: Application to trivalent TM^{3+} and Ho^{3+} in $YLiF_4$ and $LuLiF_4$ " Journal of Applied Physics Vol. **95**, No. 7 pp.3255-3271 April 2004

[14] Grady J. Koch, Jeffrey Y. Beyon, Fabien Gibert, Bruce W. Barnes, Syed Ismail, Mulugeta Petros, Paul J. Petzar, Jirong Yu, Edward A. Modlin, Kenneth J. Davis, Upendra N. Singh" Side-Line Tunable Laser Transmitter for Differential Absorption Lidar Measurements of CO2: Design and Application to Atmospheric Measurements" Applied Optics, Vol. 47 issue 7 pp.944-956, 2008

[15] G. J. Koch, M. Petros, Jirong Yu," Coherent DIAL with a Ho:Tm:YLF Laser for measurement of Wind, water vapor, and Carbon Dioxide," 11th Coherent Laser Radar Conference, Great Malvern, United Kingdom, July 2001

[16] G. J. Koch, M. Petros, J. Yu, J. Y. Beyon, B. W. Barnes, F. Amzajerdian, R. E. Davis, M. J. Kavaya, S. Ismail, and U. N. Singh, "2-□m Coherent DIAL Measurements of Atmospheric CO2," 12th Coherent Laser Radar Conference, Bar Harbor, ME (15-21 June 2003)

[17] S. Ismail, G. J. Koch, B. W. Barnes, N. Abedin, T. F. Refaat, J. Yu, S. A. Vay, S. A. Kooi, E. V. Browell, and U. N. Singh, "Technology Developments for Tropospheric Profiling of CO2 and Ground-Based Measurements," International Laser Radar Conference (ILRC) (2004)

[18] Yingxin Bai, Jirong Yu, M. Petros, Bo. Trieu, Hyung Lee, U. Singh, "High repetition rate and frequency stabilized Ho:YLF laser for CO_2 differential absorption lidar" *Advanced Solid-State Photonics 2009*, The Optical Society of America, Denver, Colorado, USA, February, 2009, WB22

[19] Menzies R. T. and D. M. Tratt, "Differential laser absorption spectrometry for global profiling of tropospheric carbon dioxide: selection of optimum sounding frequencies for high-precision measurements", Appl. Opt., **42**, 6569-6577, 2003

[20] Ambrico, P. E., A. A. Amodeo, P. D. Gilaramo, and N. Spinelli, "Sensitivity analysis of differential absorption lidar measurements in the mid-inferared region, *Appl. Opt*., **39**, 6847-6865, 2000

[21] Regalia-Jarlot, L., V. Zeninari, B. Parvitte, A. Grossel, X. Thomas, P. von der Heyden, and G. Durry "A complete study of the line intensities of four bands of CO_2 around 1.6 and 2.0 μm: A comparison between Fourier transform and diode laser measurements" *J. Quantitative Spectroscopy & Radiative Transfer* 101, (2006)325-335

[22] N. P. Barnes, W. J. Rodriguez and B. M. Walsh, "Ho:Tm:YLF laser amplifiers" J. Opt. Soc. Am. B. , **13**, 2872-

2882, (1996)
[23] B. M. Walsh, N. P. Barnes and B. Di Bartolo, "On the distributions of energy between the Tm $^3F_4$ and Ho $^5I_7$ manifolds in Tm-sensitized Ho luminescence", J. of Lum., **75**, 89-98, (1997)
[24] G. Rustad and K. Stenersen, " Modeling of laser-Pumped Tm and Ho lasers Accounting for Upconversion and Ground-state Depletion", IEEE J. Quantum Electron., **32**, 1645-1656, (1996).
[25**]** D. Bruneau, S. Delmonte and J. Pelon, "Modeling of Tm,Ho: YAG and Tm,Ho:YLF 2-μm lasers and calculation of extractable energies", App. Opt., **37**, 8406-8419, (1998).